

The Martensitic Transition and Magnetocaloric Effect of Mn-Poor MnCoGe Melt-Spun Ribbons

Yao Liu, Ming Zhang, Fengxia Hu, Jing Wang, Rongrong Wu, Yingying Zhao, Hao Kuang, Wenliang Zuo, Jirong Sun, and Baogen Shen

Beijing National Laboratory for Condensed Matter Physics, State Key Laboratory of Magnetism, Institute of Physics, Chinese Academy of Sciences, Beijing 100190, China

We investigated the martensitic transition and the magnetic properties of $Mn_{1-x}CoGe$ melt-spun ribbons. The as-prepared $Mn_{1-x}CoGe$ ribbons crystallize in austenite hexagonal phase with a textured structure. The postannealing process promotes the formation of the martensitic phase and homogenization of the alloy, resulting in a first-order magnetostructural transition in the annealed ribbons, and thus a giant magnetocaloric effect. The magnetic entropy change around the transition reaches 19 J/kgK for a magnetic field change of $0\text{--}5 \text{ T}$. Furthermore, it is found that the hysteresis loss around the magnetostructural transition is negligible in present annealed ribbons, which would facilitate the application of $Mn_{1-x}CoGe$ alloys.

Index Terms—Magnetocaloric effect (MCE), martensitic transformation, Mn–Co–Ge ribbon, rapid quenching.

I. INTRODUCTION

IN THE recent decades, MnCoGe-based alloys have widely been studied due to their intriguing behaviors relating to the giant magnetocaloric effect (MCE). The stoichiometric MnCoGe alloy crystallizes in the Ni₂In-type hexagonal structure (space group $P6_3/mmc$) and undergoes martensitic transition to TiNiSi-type orthorhombic phase (space group $Pnma$) at the structural transition temperature of 420 K upon cooling [1], [2]. The intrinsic magnetic properties are different in the two phases due to the different crystal symmetry. It is known that the magnetic moment in the alloy is mainly confined to the Mn and Co atoms, and the Mn–Mn distance is longer in the orthorhombic phase than that of the hexagonal one. As a result, the martensitic orthorhombic phase has higher Curie temperature and saturation magnetic moment ($T_C^M = 355 \text{ K}$, $M_s = 4.13 \mu_B$) than the austenite hexagonal one ($T_C^A = 265 \text{ K}$, $M_s = 2.76 \mu_B$) [2]–[4]. In other words, the stoichiometric MnCoGe alloy shows separated magnetic and structural transitions. The martensitic structural temperature (420 K) locates at the paramagnetic (PM) region, while the magnetic transition of martensitic phase occurs at a lower temperature of $T_C^M = 355 \text{ K}$.

The feature that makes MnCoGe-based alloy attractive is that the magnetic and structural transitions of the materials can be tuned to be coupled by introducing the chemical and physical pressures [5], [6]. Previous studies have demonstrated that the structural transition temperature (T_{stru}) of the alloy can be adjusted to lower temperatures by introducing chemical pressures, such as Co vacancies [7], [8], Mn vacancies [9], interstitial atoms, such as B [10], or the substitution of the main elements by the fourth elements [11]–[14], whereas the intrinsic Curie temperature T_C^A and T_C^M do not change much. When the T_{stru} is tuned to reside in the temperature window between the T_C^A and T_C^M , the coupling between the magnetic

and the structural transitions takes place, which is so-called magnetostructural transition, T_{mstr} .

The Mn-poor $Mn_{1-x}CoGe$ alloy with $0 \leq x \leq 0.05$ prepared by the conventional arc-melting technique has been previously studied [9]. The research has shown that Mn vacancies have little effect on the intrinsic Curie temperature of both the phases. The T_{stru} , on the other hand, decreases with increasing Mn vacancies, and can be modulated to reside in between the T_C^A and the T_C^M , thus inducing magnetostructural coupling within an Mn vacancy range of $0.01 < x \leq 0.045$. This paper also demonstrates that the compositions of the $Mn_{1-x}CoGe$ with coupled magnetic and structural properties show giant MCE, but a considerable magnetic hysteresis is accompanied.

Melt spinning is an important technique to fabricate alloys. This technique has the advantages of getting fine grains, textured structure, and can also promote the homogenization of the alloy, thus shortening the annealing time. There has been a lot of studies on the martensitic transition, magnetic properties, and MCE of the melt-spun ribbons with the martensitic transition, including NiMn-based Heusler alloys [15]–[18]. However, MnCoGe-based alloys that also have a promise in MCE, as discussed above, were rarely studied in the form of the melt-spun ribbons [19].

Here, we report the structure, magnetic properties, and MCE of Mn-poor $Mn_{1-x}CoGe$ ribbons prepared by the melt-spinning technique. The as-prepared ribbons crystallize in the hexagonal phase, and the martensitic transition was suppressed. After annealing at 1123 K for 1 h, the ribbons show a coupled nature of the structural and magnetic properties with giant MCE. Compared with the $Mn_{1-x}CoGe$ bulk prepared by the conventional arc-melting technique [9], the annealing time of the melt-spun ribbons has been largely shortened and the magnetic hysteresis significantly reduced.

II. EXPERIMENT

The primary $Mn_{1-x}CoGe$ alloys with the nominal compositions of $Mn_{0.99}CoGe$ ($x = 0.01$) and $Mn_{0.98}CoGe$ ($x = 0.02$)

Manuscript received March 20, 2015; accepted June 17, 2015. Date of publication June 23, 2015; date of current version October 22, 2015. Corresponding author: F. Hu (e-mail: fxhu@iphy.ac.cn).

Color versions of one or more of the figures in this paper are available online at <http://ieeexplore.ieee.org>.

Digital Object Identifier 10.1109/TMAG.2015.2448654

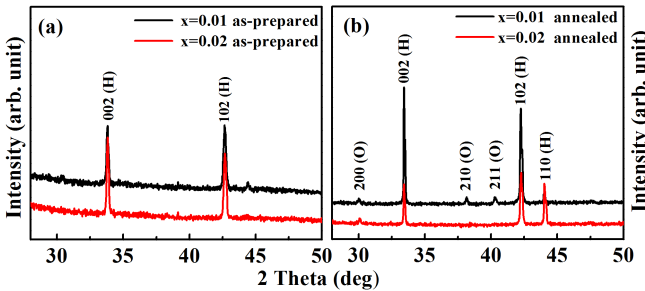


Fig. 1. Room temperature XRD patterns of (a) as-prepared and (b) annealed ribbons with both $x = 0.01$ and $x = 0.02$. Miller indices (hkl): Ni₂In-type hexagonal (H) and TiNiSi-type orthorhombic (O) structure.

were prepared through the arc-melting technique under the protection of Ar atmosphere from the raw elements of Mn, Co, and Ge with purities better than 99.9%. The ingots were then cut into appropriate pieces and inserted into a quartz tube with a nozzle, induction melted under the protection of Ar atmosphere, and finally ejected onto a rotating copper wheel via a pressure difference. The speed of the copper wheel was 20 m/s. The possible Mn loss during the fabrication process was not compensated for the starting materials. For the arc-melted ingots, if we assume Mn is the only element that experiences loss during the arc-melting process, the estimated compositions of the resulted ingots were Mn_{0.971}CoGe and Mn_{0.963}CoGe for primary $x = 0.01$ and $x = 0.02$, respectively. Some of the as-prepared ribbons were then wrapped in pieces of Mo foil, and sealed into an evacuated quartz tube, annealed at 1123 K for an hour and quenched in water subsequently. The room temperature X-ray diffraction (XRD) patterns for the samples were measured using Cu-K α radiation. The magnetic properties were measured using the quantum design a superconducting quantum interference device (SQUID-VSM) system.

III. RESULTS AND DISCUSSION

The room temperature XRD patterns of the as-prepared ribbons with the nominal compositions of both $x = 0.01$ and $x = 0.02$ are displayed in Fig. 1(a). One can notice that the as-prepared ribbons with both the compositions crystallize in the Ni₂In-type hexagonal structure. Furthermore, the XRD patterns also indicate that the as-prepared ribbons show a texture mainly with (00l) direction oriented vertically to the ribbon plane, noting the enhanced peaks corresponding to the (002) and (102) hexagonal structure. After the ribbons were annealed at 1123 K for 1 h, the orthorhombic structure emerged at room temperature, as shown in the XRD pattern in Fig. 1(b), for the ribbons with $x = 0.01$. The martensitic and austenite phases coexist at room temperature, implying that the martensitic transition locates around the room temperature. Otherwise, the ribbons with $x = 0.02$ still crystallize in the single hexagonal structure, which means that the martensitic transition should be lower than the room temperature.

Fig. 2(a) shows the magnetization dependence on temperature ($M-T$ curves) for the as-prepared and annealed Mn_{1-x}CoGe ribbons with the nominal compositions of $x = 0.01$ and 0.02 measured in the zero-field-cooling (ZFC) and FC modes under a magnetic field of 0.05 T. The differentiation of magnetization with respect to temperature

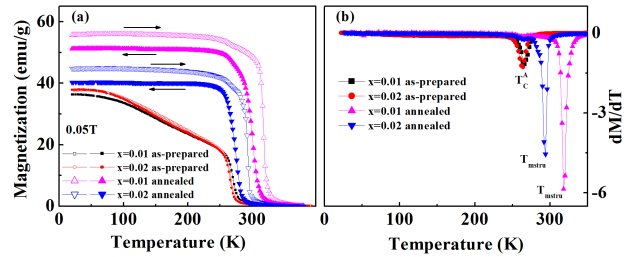


Fig. 2. (a) $M-T$ curves of the as-prepared and annealed ribbons measured in a magnetic field of 0.05 T for Mn_{1-x}CoGe ($x = 0.01$ and $x = 0.02$). Open symbol: ZFC mode. Solid symbol: FC mode process. Arrows: heating and cooling process. (b) Differentiation of magnetization with respect to temperature (dM/dT) for the as-prepared and annealed ribbons with $x = 0.01$ and $x = 0.02$.

(dM/dT plots) on heating for the as-prepared and annealed ribbons is shown in Fig. 2(b). The temperature corresponding to the minimum in the plot refers to the magnetic transition temperature of the materials. The $M-T$ curves of the as-prepared ribbons with both the compositions almost coincide with each other, denoting a similar transition around 266 K. This temperature happens to be the same as the Curie temperature T_C^A of the austenitic phase [1]–[4], and the transitions are completely reversible for the heating and cooling process. This fact indicates that the martensitic structural transition is suppressed, and only a second-order magnetic transition occurs around T_C^A for the as-prepared ribbons. The exact reason for the suppression of the martensitic transition is unclear. However, it should be closely related to the formation of textured structure, possible stress, as well as the possible inhomogeneities during the melt-spinning process, noting that all these factors may depress the nucleation of the martensitic phase on cooling.

It is intriguing that the $M-T$ curves of the annealed ribbons show quite different behaviors from the as-prepared ones. Sharp transition between the FM and PM states with pronounced thermal hysteresis takes place. The transition temperatures are determined from the dM/dT plot as 318 and 294 K, while the hysteresis gap is 19 and 21 K for the ribbons with $x = 0.01$ and $x = 0.02$, respectively. The large thermal hysteresis is evidence of the first-order nature of the transitions. The magnetostructural coupling is thus realized in the annealed ribbons. Due to the coupled nature of the magnetic and structural transitions, a large MCE can be expected. These results denote that the annealing process may have promoted the homogenization and reduced the possible stress and textured structure introduced in the ribbons during the melt-spinning process. Furthermore, in contrast to the long annealing time for the arc-melted alloys (usually several days), the annealing process is largely shortened for the melt-spun ribbons. In Fig. 3, the $M-T$ curves for annealed ribbons with both the compositions in a high magnetic field of 5 T are displayed. The magnetization shows a sharp change around the transition, which further confirms the magnetostructural transition for the annealed ribbons.

For the present Mn_{1-x}CoGe ribbons, the origin for the modulation of T_{str} by Mn vacancies should be the same as that for the arc-melted ones. It is known that the Co atoms in

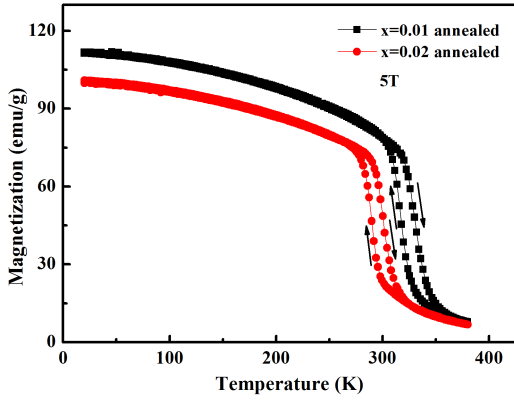


Fig. 3. M - T curves of the annealed ribbons measured in a high magnetic field of 5 T for $x = 0.01$ and $x = 0.02$. Arrows: heating and cooling process.

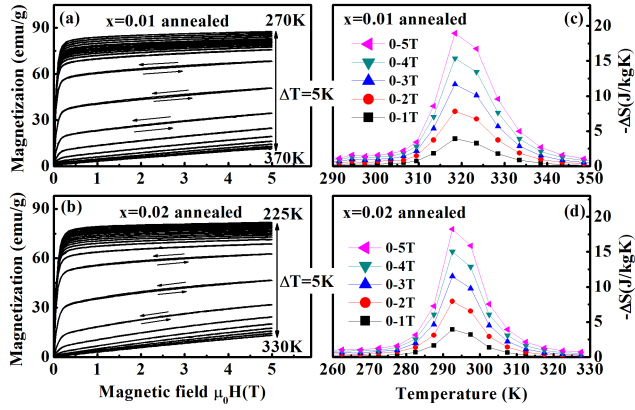


Fig. 4. Isothermal magnetization curves for the annealed ribbons with (a) $x = 0.01$ and (b) $x = 0.02$. Arrows: ascending and descending process of the magnetic field during the measurement. Magnetic entropy change as a function of temperature under different magnetic fields for the annealed ribbons with (c) $x = 0.01$ and (d) $x = 0.02$.

the arc-melted $Mn_{1-x}CoGe$ alloys can occupy the Mn vacancies and thus result in Co vacancies [8], [20]. The effect of Co vacancies on the martensitic transition has been studied both experimentally and theoretically [7], [8], [21]. The *ab initio* calculation demonstrates that the Co vacancies can change the structural symmetry and modify the coupling distance between the Mn–Mn atoms [21], which agrees well with the experimental studies on the $MnCo_{1-x}Ge$ [8]. Thus, by introducing Mn vacancies, the T_{stru} can be tuned to lower temperature by adjusting structural symmetry and Mn–Mn distance in the $Mn_{1-x}CoGe$ alloys. Another factor that affects the T_{stru} is the valence-electron concentration, e/a, the reduction of e/a usually drives the T_{stru} to lower temperature [22]. In the arc-melted $Mn_{1-x}CoGe$ alloys, it was found that the Curie temperature of both the phases remains almost unchanged, while T_{stru} decreases with the reduction of e/a. This also works for the $Mn_{1-x}CoGe$ ribbons.

The isothermal magnetization curves of the annealed ribbons for $x = 0.01$ and $x = 0.02$ are shown in Fig. 4. These curves were measured with the magnetic field applied along the ribbon plane. It is worth emphasizing here that the

magnetic hysteresis is negligible for the annealed ribbons. This phenomenon is quite different from that of the arc-melted $Mn_{1-x}CoGe$ alloy with the first-order magnetostructural transition, in which a significantly large magnetic hysteresis with hysteresis loss of 207 J/kg around the T_{mstru} of 292 K was observed in a magnetic field of 14 T [9]. For most of the first-order transition systems, both the magnetic and thermal hysteresis usually appear simultaneously. The different hysteresis behavior in thermal and magnetic field cycles may imply a different nucleation mechanism under different external perturbations. For present annealed ribbons, the thermal hysteresis reaches 19 and 21 K for $x = 0.01$ and $x = 0.02$, respectively, whereas no obvious magnetic hysteresis is observed. This fact indicates that the magnetic field may be not an effective way to induce the martensitic transition between the PM hexagonal and FM martensitic phases for the annealed melt-spun ribbons. In other words, the energy barrier during the transition can be overcome easily by thermal activation rather than by the field-induced spin-lattice coupling in the annealed ribbons. The factors related to hysteresis behavior can be both intrinsic and extrinsic [23], [24]. The extrinsic ones refer to the thermal equilibrium and the situation of heat transfer during the measurement, which is related to the sweep rate of temperature and magnetic field. The intrinsic ones, on the other hand, usually relate to the band structure, impurity, nucleation factors, and strain effect. The exact reason why the arc-melted alloys show large magnetic hysteresis around the martensitic transition, while the annealed ribbons display almost negligible hysteresis, is unclear. However, since the ribbons have different microstructures, grain distributions, and internal stress from the arc-melted alloys, the change of band structure, and thus the different nucleation mechanisms, should be possible although the specific reason still needs further investigations.

Based on the isothermal magnetization curves of the annealed ribbons, the temperature dependence of magnetic entropy change [$\Delta S_M(T)$] for both $x = 0.01$ and $x = 0.02$ due to a magnetic field change (ΔB) up to 5 T is calculated using the Maxwell relation, and the results are shown in Fig. 4. One can find that the absolute magnetic entropy change reaches 8 J/kgK for ΔB of 2 T and 18 J/kgK for ΔB of 5 T around the T_{mstru} for the annealed ribbons with $x = 0.02$. These results are approaching the reported maximum ΔS_M for the arc-melted Mn-poor $Mn_{1-x}CoGe$ bulk, which is 10 J/kgK for ΔB of 2 T and 26 J/kgK for ΔB of 5 T [9]. These ΔS_M values were also evaluated using the same way.

To evaluate the MCE of a material, there are two more parameters that need to be considered, i.e., the refrigerant capacity (RC) and the hysteresis loss. RC is a measure of the energy that a refrigerant can transfer between the hot and cold sources. It is defined as $RC = \int_{T_2}^{T_1} |\Delta S(T)|_{\Delta H} dH$ [25], where T_1 and T_2 are the temperatures corresponding to the full-width at half-maximum in the $|\Delta S_M(T)|$ curves. For ΔB of 5 T, the obtained RC for the annealed ribbons with $x = 0.02$ is 207.6 J/kg, whereas the evaluated RC using the same for the arc-melted alloys is ~ 183.5 J/kg under 5 T. Usually, the effective RC (RC_{eff}) of a material can be

obtained by subtracting the hysteresis loss from RC, so the RC_{eff} of a material with the first-order transition is restricted by the hysteresis loss. Normally, the hysteresis loss can be obtained by calculating the area enclosed by the ascending and descending plots in the magnetization curves. In the arc-melted $Mn_{1-x}CoGe$ alloys [9], the hysteresis loss around the transition temperature in a magnetic field of 14 T reaches 206 J/kg. Such a considerable loss will reduce the RC_{eff} largely. On the contrary, the magnetic hysteresis is negligible in the annealed ribbons as seen in the $M(H, T)$ curves, so the hysteresis loss is approximately zero. As a result, the annealed ribbons will show an enhanced RC_{eff} , which facilitates the application of the alloys.

ACKNOWLEDGMENT

This work was supported in part by the National Basic Research Program of China (973 Program) under Grant 2014CB643700 and Grant 2012CB933000, in part by the National Natural Science Foundation of China under Grant 51271196, Grant 11274357, and Grant 11174345, in part by the Beijing Natural Science Foundation under Grant 2152034, and in part by the Strategic Priority Research Program (B) through the Chinese Academy of Sciences, Beijing, China, under Grant XDB07030200.

REFERENCES

- [1] S. Nizioł, A. Wesełucha, W. Bażela, and A. Szytuła, "Magnetic properties of the $Co_xNi_{1-x}MnGe$ system," *Solid State Commun.*, vol. 39, no. 10, pp. 1081–1085, 1981.
- [2] V. Johnson, "Diffusionless orthorhombic to hexagonal transitions in ternary silicides and germanides," *Inorganic Chem.*, vol. 14, no. 5, pp. 1117–1120, 1975.
- [3] S. Kaprzyk and S. Nizioł, "The electronic structure of $CoMnGe$ with the hexagonal and orthorhombic crystal structure," *J. Magn. Magn. Mater.*, vol. 87, no. 3, pp. 267–275, 1990.
- [4] S. Lin, O. Tegus, E. Brück, W. Dagula, T. J. Gortenmulder, and K. H. J. Buschow, "Structural and magnetic properties of $MnFe_{1-x}Co_xGe$ compounds," *IEEE Trans. Magn.*, vol. 42, no. 11, pp. 3776–3778, Nov. 2006.
- [5] T. Kanomata, H. Ishigaki, T. Suzuki, H. Yoshida, S. Abe, and T. Kaneko, "Magneto-volume effect of $MnCo_{1-x}Ge(0 \leq x \leq 0.2)$," *J. Magn. Magn. Mater.*, vols. 140–144, pp. 131–132, Feb. 1995.
- [6] S. Anzai and K. Ozawa, "Coupled nature of magnetic and structural transition in $MnNiGe$ under pressure," *Phys. Rev. B*, vol. 18, p. 2173, Sep. 1978.
- [7] Y.-K. Fang, J.-C. Yeh, W.-C. Chang, X.-M. Li, and W. Li, "Structures, magnetic properties, and magnetocaloric effect in $MnCo_{1-x}Ge$ ($0.02 \leq x \leq 0.2$) compounds," *J. Magn. Magn. Mater.*, vol. 321, pp. 3053–3056, Oct. 2009.
- [8] K. Koyama, M. Sakai, T. Kanomata, and K. Watanabe, "Field-induced martensitic transformation in new ferromagnetic shape memory compound $Mn_{1.07}Co_{0.92}Ge$," *Jpn. J. Appl. Phys.*, vol. 43, no. 12, p. 8036, 2004.
- [9] E. K. Liu *et al.*, "Vacancy-tuned paramagnetic/ferromagnetic martensitic transformation in Mn-poor $Mn_{1-x}CoGe$ alloys," *Eur. Phys. Lett.*, vol. 91, no. 1, p. 17003, 2010.
- [10] N. T. Trung, L. Zhang, L. Caron, K. H. J. Buschow, and E. Brück, "Giant magnetocaloric effects by tailoring the phase transitions," *Appl. Phys. Lett.*, vol. 96, no. 17, p. 172504, 2010.
- [11] S. C. Ma *et al.*, "Large room temperature magnetocaloric effect with negligible magnetic hysteresis losses in $Mn_{1-x}V_xCoGe$ alloys," *J. Magn. Magn. Mater.*, vol. 324, no. 2, pp. 135–139, 2012.
- [12] N. T. Trung, V. Biharie, L. Zhang, L. Caron, K. H. J. Buschow, and E. Brück, "From single- to double-first-order magnetic phase transition in magnetocaloric $Mn_{1-x}Cr_xCoGe$ compounds," *Appl. Phys. Lett.*, vol. 96, no. 16, p. 162507, 2010.
- [13] J. B. A. Hamera, R. Daou, S. Özcan, N. D. Mathur, D. J. Fray, and K. G. Sandeman, "Phase diagram and magnetocaloric effect of $CoMnGe_{1-x}Sn_x$ alloys," *J. Magn. Magn. Mater.*, vol. 321, no. 21, pp. 3535–3540, 2009.
- [14] L. F. Bao *et al.*, "Evolution of magnetostructural transition and magnetocaloric effect with Al doping in $MnCoGe_{1-x}Al_x$ compounds," *J. Phys. D, Appl. Phys.*, vol. 47, no. 5, p. 055003, 2014.
- [15] A. K. Panda, M. Ghosh, A. Kumar, and A. Mitra, "Magnetic transitions and structure of a NiMnGa ferromagnetic shape memory alloy prepared by melt spinning technique," *J. Magn. Magn. Mater.*, vol. 320, no. 17, pp. L116–L120, 2008.
- [16] J. L. S. Llamazares *et al.*, "Martensitic phase transformation in rapidly solidified $Mn_50Ni_{40}In_{10}$ alloy ribbons," *Appl. Phys. Lett.*, vol. 92, no. 1, p. 012513, 2008.
- [17] B. Hernando *et al.*, "Magnetocaloric effect in preferentially textured $Mn_50Ni_{40}In_{10}$ melt spun ribbons," *Appl. Phys. Lett.*, vol. 94, no. 22, p. 222502, 2009.
- [18] O. Hečko, P. Švec, D. Janíković, and K. Ullakko, "Magnetic properties of Ni-Mn-Ga ribbon prepared by rapid solidification," *IEEE Trans. Magn.*, vol. 38, no. 5, pp. 2841–2843, Sep. 2002.
- [19] C. F. Sanchez-Valdes, J. L. S. Llamazares, H. Flores-Zuniga, D. Rios-Jara, P. Alvarez-Alonso, and P. Gorria, "Magnetocaloric effect in melt-spun $MnCoGe$ ribbons," *Scripta Mater.*, vol. 69, no. 3, pp. 211–214, 2013.
- [20] W. Jeitschko, "A high-temperature X-ray study of displacive phase transition in $MnCoGe$," *Acta Cryst. B*, vol. 31, pp. 1187–1190, 1975.
- [21] T.-J. Wang *et al.*, "Vacancy induced structural and magnetic transition in $MnCo_{1-x}Ge$," *Appl. Phys. Lett.*, vol. 89, no. 26, p. 262504, 2006.
- [22] T. Samanta, I. Dubenko, A. Quetz, S. Temple, S. Stadler, and N. Ali, "Magnetostructural phase transitions and magnetocaloric effects in $MnNiGe_{1-x}Al_x$," *Appl. Phys. Lett.*, vol. 100, no. 5, p. 052404, 2012.
- [23] J. D. Moore, K. Morrison, K. G. Sandeman, M. Katter, and L. F. Cohen, "Reducing extrinsic hysteresis in first-order $La(Fe,Co,Si)_{13}$ magnetocaloric systems," *Appl. Phys. Lett.*, vol. 95, no. 25, p. 252504, 2009.
- [24] F. X. Hu, L. Chen, J. Wang, F. L. Bao, J. R. Sun, and B. G. Shen, "Particle size dependent hysteresis loss in $La_{0.7}Ce_{0.3}Fe_{11.6}Si_{1.4}C_{0.2}$ first-order systems," *Appl. Phys. Lett.*, vol. 100, no. 7, p. 072403, 2012.
- [25] K. A. Gschneidner, Jr., V. K. Pecharsky, A. O. Pecharsky, and C. B. Zimm, "Recent developments in magnetic refrigeration," *Mater. Sci. Forum*, vol. 315, pp. 69–76, Jul. 1999.